Available online at www.sciencedirect.com

ScienceDirect

Physics Procedia 65 (2015) 177 – 180

Physics Procedia

27th International Symposium on Superconductivity, ISS 2014

Quantum Interference in DC-SQUIDs Comprising Two Sub-Micron Aluminum Josephson Junctions: Deviation from Classical Model

Koji Miura, Kento Kikuchi, Hiroshi Shimada, Yoshinao Mizugaki*

Department of Engineering Science, The University of Electro-Communications, 1-5-1 Chofugaoka, Chofu, Tokyo, 182-8585, Japan

Abstract

In a small Josephson junction, the critical current is often found experimentally to be smaller than the value expected from the Ambegaokar-Baratoff theory because of the quantum phase fluctuations. We also observed in our previous study that the quantum interference in a dc-SQUID comprising sub-micron Al junctions deviated from the classical model. In this work, we have fabricated 13 devices having different values of maximal critical currents, and evaluated their quantum interference patterns. The quantum interference of 12 among 13 devices has deviated from the classical model. It is confirmed that their maximal critical currents ($I_{csq,max}$) are reduced from the values (I_{csq0}) predicted by the Ambegaokar-Baratoff theory. Besides, the quantum interference for $I_{csq,max}$ / I_{csq0} < 0.4 agrees with the modified quantum-interference model.

Peer-review under responsibility of the ISS 2014 Program Committee

Keywords: Al/AlO_x/Al tuunel junction; Josephson junction; quantum interference; quantum phase fluctuations; charging energy

1. Introduction

Sub-micron Al/AlO_x/Al tunnel junctions are employed in quantum devises such as superconducting qubits [1] and single-electron (single-Cooper-pair) devices [2, 3]. Their electrical characteristics are influenced by the charging energy of a single electron, E_c, owing to their small junction capacitances. In a small Josephson junction, in which E_c cannot be ignored, the critical current I_c is often found experimentally to be smaller than the value (I_{c0}) expected from the Ambegaokar-Baratoff theory [4] due to the quantum phase fluctuations. It is empirically known that I_c decreases from I_{c0} with decreasing the energy ratio E_J / E_c, which is expressed by [5]

$$\frac{I_c}{I_{c0}} = \left(\frac{1}{\pi^2}\right)\left(\frac{2E_J}{E_c}\right)^{0.5} . \quad (1)$$

* Corresponding author. Tel.:+81-42-443-5437; fax: +81-42-443-5437.
E-mail address: y.mizugaki@uec.ac.jp

Peer-review under responsibility of the ISS 2014 Program Committee
doi:10.1016/j.phpro.2015.05.104

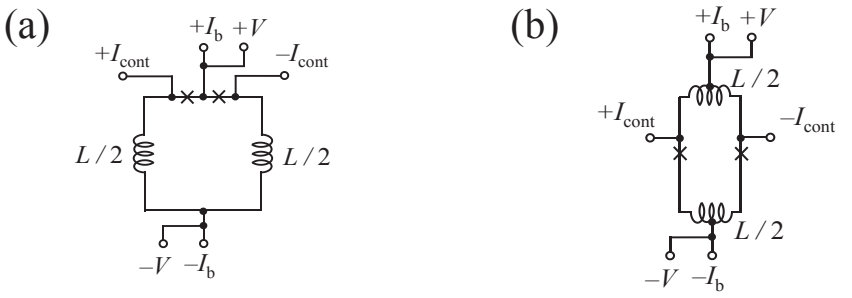

Figure 1 Equivalent circuit models of fabricated dc-SQUIDs. (a) Type I. (b) Type II.

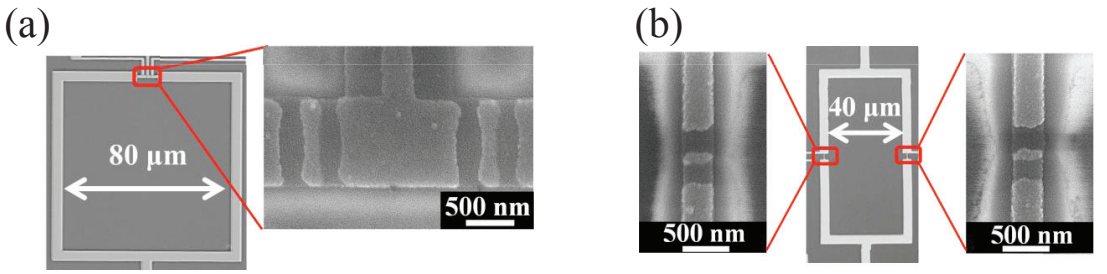

Figure 2 Optical and scanning electron micrographs of fabricated devices. (a) Sample B. (b) Sample F_No.1.

In our previous work, we also observed that the quantum interference patterns of a superconducting quantum interference device (dc-SQUID) comprising two sub-micron Al junctions deviated from the classical model [6]. We proposed a modified quantum-interference model that included the effect of quantum phase fluctuations. It is given by

$$I_{csq} = 2I_{cJ}\left|\cos\frac{\pi LI_{cont}}{\Phi_0}\right|^{1/(1-m)} . \quad (2)$$

Here I_{csq}, I_{cJ}, Φ_0, L, and I_{cont} are the critical current of the dc-SQUID, the critical current of each Josephson junction, a flux quantum, the loop inductance, and the control current modulating I_{csq}, respectively. m is the parameter taking account of the effect of quantum phase fluctuations, where we assume $2I_{cJ} \propto (I_{csq})^m$. m is zero in the classical model. From the quantum phase fluctuations given by Eq. (1), m is derived to be 0.5 for a dc-SQUID comprising small Josephson junctions. In fact, we obtained better fitting to the experimental data of one device. In this work, we attempt to figure out the boundary between the classical and the modified model: we have fabricated 13 devices having different values of maximal critical currents and evaluated their quantum interference patterns.

2. Sample Fabrication and Measurement Setup

Devices were fabricated on a thermally oxidizes Si substrates using *e*-beam lithography and Al shadow evaporation [7]. We have designed two types of dc-SQUIDs (Types I and II) with different loop areas. Figures 1(a) and 1(b) show the equivalent circuits of Types I and II, respectively. The loop area of Type II is approximately a half of that of Type I. Two devices of Type II were fabricated on the same chip, whereas one device of Type I was placed on one chip. I_{csq} is modulated by applying I_{cont} directly to the SQUID loop.

The maximal values of critical currents $I_{csq,max}$ were varied by changing junction areas and oxidation conditions. We measured 8 devices of Type I and 5 devices of Type II. Figures 2(a) and 2(b) show optical and scanning electron micrographs of the devices B (Type I) and F_No.1 (Type II), respectively.

Measurements were conducted at around 100 mK in a compact dilution refrigerator [8]. All measurement leads had low-pass filters at room temperature and distributed RLC low-pass filters between the 1 K stage and the mixing chamber in order to reduce electrical noise. In the measurement, the bias voltage was applied symmetrical to the device.

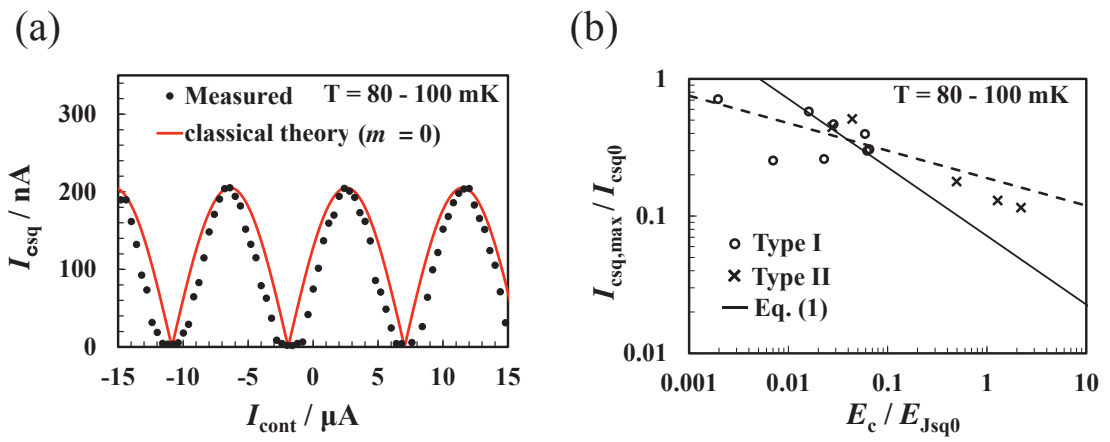

Figure 3 (a) Quantum interference pattern of device B. The solid curve represents the classical model given by Eq. (2) with $m = 0$. (b) Dependence of the normalized maximal critical current $I_{csq,max}$ / I_{csq0} on the energy ratio E_c / E_{Jsq0}. The solid line represents Eq. (1) and the dashed line shows the fitting result.

For Type I, the junction capacitance C was obtained using the SQUID resonance step and the quantum interference period. On the other hand, for Type II, we estimated C from the dependence of the specific capacitance on the specific normal conductance which we had obtained in our previous studies.

3. Results and Discussion

Figure 3(a) shows the quantum interference pattern of the device B. It is found that the measured values of I_{csq} are smaller than the values obtained from the classical model. In other words, I_{csq} decreases rapidly from the maximal value. Such deviation from the classical model is observed clearly in 12 out of 13 devices.

Figure 3(b) shows the normalized maximal critical currents $I_{csq,max}$ / I_{csq0} of all devices plotted as functions of the energy ratios E_c / E_{Jsq0}, where E_{Jsq0} is the Josephson coupling energy obtained using the Ambegaokar-Baratoff relationship [4]. It is confirmed that $I_{csq,max}$ decreases from I_{csq0} with increasing E_c / E_{Jsq0}. However, the measured values tend to be larger than the values predicted from Eq. (1). The dashed line shows the fitting result of $I_{csq,max}$ / I_{csq0} ∝ $(E_{Jsq0} / E_c)^{0.20}$. It is suggested that the effect of the quantum phase fluctuations is less than that in a small junction, since the two junctions are connected through a large loop.

Although the quantum interference of 12 devices has deviated from that of the classical model, the degrees of deviation are different for each device. In order to evaluate the quantum interference in detail, the normalized critical currents I_{csq} / I_{csq0} of 3 devices are plotted in Fig. 4(a) as functions of the effective energy ratio E_J^{eff} / E_c. (The device parameters are listed in Table I.) The effective Josephson coupling energy E_J^{eff} is modulated by I_{cont}, which is expressed as

$$E_J^{eff} = E_{Jsq0}\left|\cos\frac{\pi L I_{cont}}{\Phi_0}\right| \quad . \tag{3}$$

The normalized critical current of the device A with the largest $I_{csq,max}$ tends to follow the classical model represented by solid line ($m = 0$). On the other hand, those of the devices B and F_No.1 have slopes steeper than the classical model, which means that I_{csq} / I_{csq0} decreases rapidly with decreasing E_J^{eff} / E_c. The parameter m is calculated using the envelopes of upper parts (70% from the maximum) data, which are plotted in Fig. 4(b) as functions of I_{csq} / I_{csq0}. m tends to increase with decreasing I_{csq} / I_{csq0}. It is confirmed that the m values are likely to converge to 0.5 for $I_{csq,max}$ / $I_{csq0} < 0.4$.

4. Conclusion

In conclusion, we fabricated dc-SQUIDs comprising two sub-micron Al tunnel junctions. The quantum interference of 12 among 13 devices had deviated from that of the classical model. Owing to the quantum fluctuations, the normalized maximal critical current, $I_{csq,max}$ / I_{csq0}, decreased with increasing E_c / E_{Jsq0} although the dependence is less than Eq. (1). For the normalized critical currents in the interference patterns (I_{csq} / I_{csq0}), on the other hand, their dependence on E_J^{eff} / E_c agrees quantitatively with the modified quantum-interference model when $I_{csq,max}$ / $I_{csq0} < 0.4$.

Table I Device parameters of device A, B and F_No.1

Device	Critical current $I_{csq,max}$ / nA	Normal resistance R_n / kΩ	Junction area S / μm^2	Loop indautance L / pH	Capacitance C / fF	Josephson coupling energy E_{Jsq0} / μeV	Charging energy E_c / μeV
A	660	0.339	0.45	304	43.0	1910	3.73
B	205	0.837	0.169	231	13.7	733	11.7
F_No.1	2.27	16.3	0.025	152	1.8	40.4	89

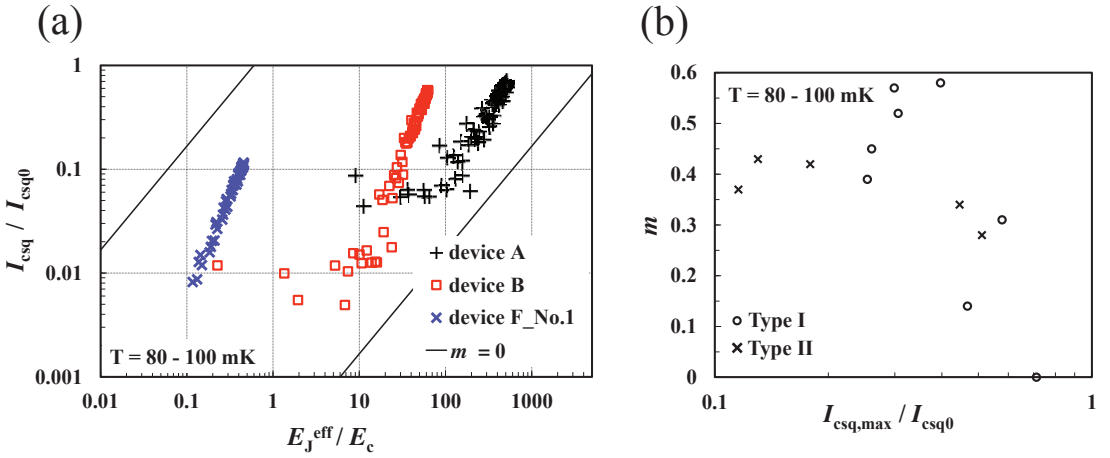

Figure 4 (a) Dependence of the normalized critical current I_{csq} / I_{csq0} on the effective energy ratio E_J^{eff} / E_c. The solid lines represents the classical model (m = 0). (b) Dependence of the parameter m on the normalized maximal critical current $I_{csq,max}$ / I_{csq0}.

Acknowledgements

The authors would like to thank K. Takeda, K. Miyawaki, and M. Moriya for fruitful discussion and technical supports.

References

[1] Y. Nakamura, Yu.A. Pashkin, J.S. Tsai, Nature 398 (1999) 786–788.
[2] H. Brenning, S. Kubatkin, P. Delsing, J. Appl. Phys.96 (2004) 6822–6826.
[3] P. Joyez, P. Lafarge, A. Filipe, D. Esteve, and M.H. Devoret, Phys. Rev. Lett. 72 (1994) 2458–2461.
[4] V. Ambegaokar, A. Baratoff, Phys. Rev. Lett. 10 (1963) 486–489.
[5] M. Tinkham, Josephson effect in low-capacitance tunnel junctions, in: H.Grabert, M.H Devoret (Eds.), Single Charge Tunnelinng, Plenum Press, New York, 1992 pp. 139–166.
[6] Y. Mizugaki, K.Kikuchi, M. Moriya, H. Shimada, Physica C 484 (2013) 206–208.
[7] G.J. Dolan, Appl. Phys. Lett. 31 (1977) 337–339.
[8] Y. Ootuka, T. Uchiyama, H. Shimada, Cryogenics 33 (1993) 923–925.